JOURNAL OF MAGNETIC RESONANCE, Series B **113,** 272–276 (1996)
ARTICLE NO. 0188

NMR Pulse Schemes for the Sequential Assignment of Arginine Side-Chain H^{ϵ} Protons

N. SAMBASIVA RAO,* PASCALE LEGAULT,* D. R. MUHANDIRAM,* JACK GREENBLATT,†
JOHN L. BATTISTE,‡ JAMES R. WILLIAMSON,‡ AND LEWIS E. KAY*

*Protein Engineering Network Centers of Excellence and Departments of Molecular and Medical Genetics, Biochemistry and Chemistry, University of Toronto, Toronto, Ontario, Canada, M5S 1A8; †Banting and Best Department of Medical Research and Department of Molecular and Medical Genetics, University of Toronto, Toronto, Ontario, Canada, M5G 1L6; and ‡Department of Chemistry, Massachusetts Institute of Technology, Cambridge, Massachusetts 02139

Received October 17, 1996

Recent developments in multidimensional, multinuclear NMR methods have greatly increased the scope of proteins and nucleic acids that can be studied by this technology (*1*). One particularly promising area of investigation relates to structural studies of protein–RNA interactions and a number of NMR-derived structures of such complexes have been reported in the past few years (*2–4*). Accurate structures of these molecular complexes depend on the assignment of intermolecular NOEs correlating proximal protein and nucleic acid spins. A key residue in stabilizing protein–nucleic acid interactions is arginine (*4, 5*). In fact, statistical analyses of protein structures establish that arginine is one of the three most abundant amino acids at molecular interfaces (*6*). Furthermore, arginines play a critical role in RNA recognition, especially in proteins with arginine-rich motifs such as TAT and REV from HIV, the N proteins from lambdoid phages, and many viral and ribosomal proteins (*7, 8*). Additionally, site-specific substitutions of arginine for lysine in a number of proteins have been shown to enhance stability, suggesting that arginine residues might serve as stabilizing elements in proteins (*9*).

Given the importance of arginine residues, it is clearly necessary that methods be developed for the unambiguous assignment of arginine side-chain chemical shifts, with focus on the guanadino group in particular, since many of the molecular interactions involve contacts with this moiety. Several years ago, Yamazaki *et al.* developed experiments for correlating arginine H^{ϵ}, N^{ϵ}, and C^{ζ} chemical shifts employing exclusively magnetization transfer via scalar connectivities (*10*). Subsequently, Wittekind and co-workers demonstrated that it is possible to observe (H^{ϵ}, N^{ϵ}, H^{δ}) correlations in the HNHA-gly experiment (*11*) and Boelens *et al.* developed a scheme for correlating guanidino H^{ϵ}, N^{η} chemical shifts (*12*). Finally, Yamazaki and co-workers have recently developed a family of experiments for sequence-specific assignment of arginine guanidino ^{15}N and ^{1}H chemical shifts (*13*).

Our interest in developing further methodology for arginine side-chain assignment was peaked during structural studies of an HIV-1 Rev peptide in complex with stem–loop IIB of the Rev response element (RRE) RNA (*4*). Eleven of the 23 residues in the Rev peptide are arginines and many make specific contacts with bases on the RNA or are in position to establish electrostatic or hydrogen-bonding interactions with the phosphate backbone of the nucleic acid (*4*). Not surprisingly, in some cases it has been difficult to link H^{ϵ} protons with the aliphatic part of the side chain on the basis of experiments which correlate H^{δ} and H^{ϵ} chemical shifts (*13*). The difficulty arises in cases where the H^{δ} shifts of one residue overlap with those of another, or where cross peaks are simply absent. With this in mind, we present a number of experiments which correlate the guanidino H^{ϵ} proton with either arginine aliphatic side-chain-carbon or -proton chemical shifts. The large numbers of potential ali-

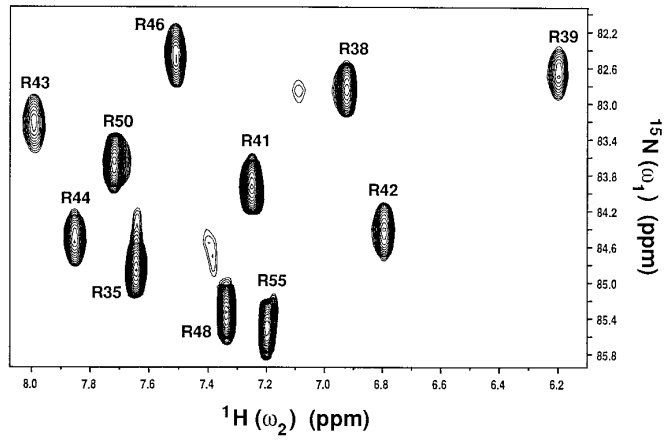

FIG. 1. Portion of the $^{1}H-^{15}N$ HSQC spectrum of the 1:1 complex of a 1.5 m*M* sample of ^{15}N, ^{13}C-labeled HIV-1 Rev peptide–RRE RNA illustrating the excellent dispersion that is often present in the (N^{ϵ}, H^{ϵ}) region of correlation maps recorded for RNA–peptide complexes.

1064-1866/96 $18.00

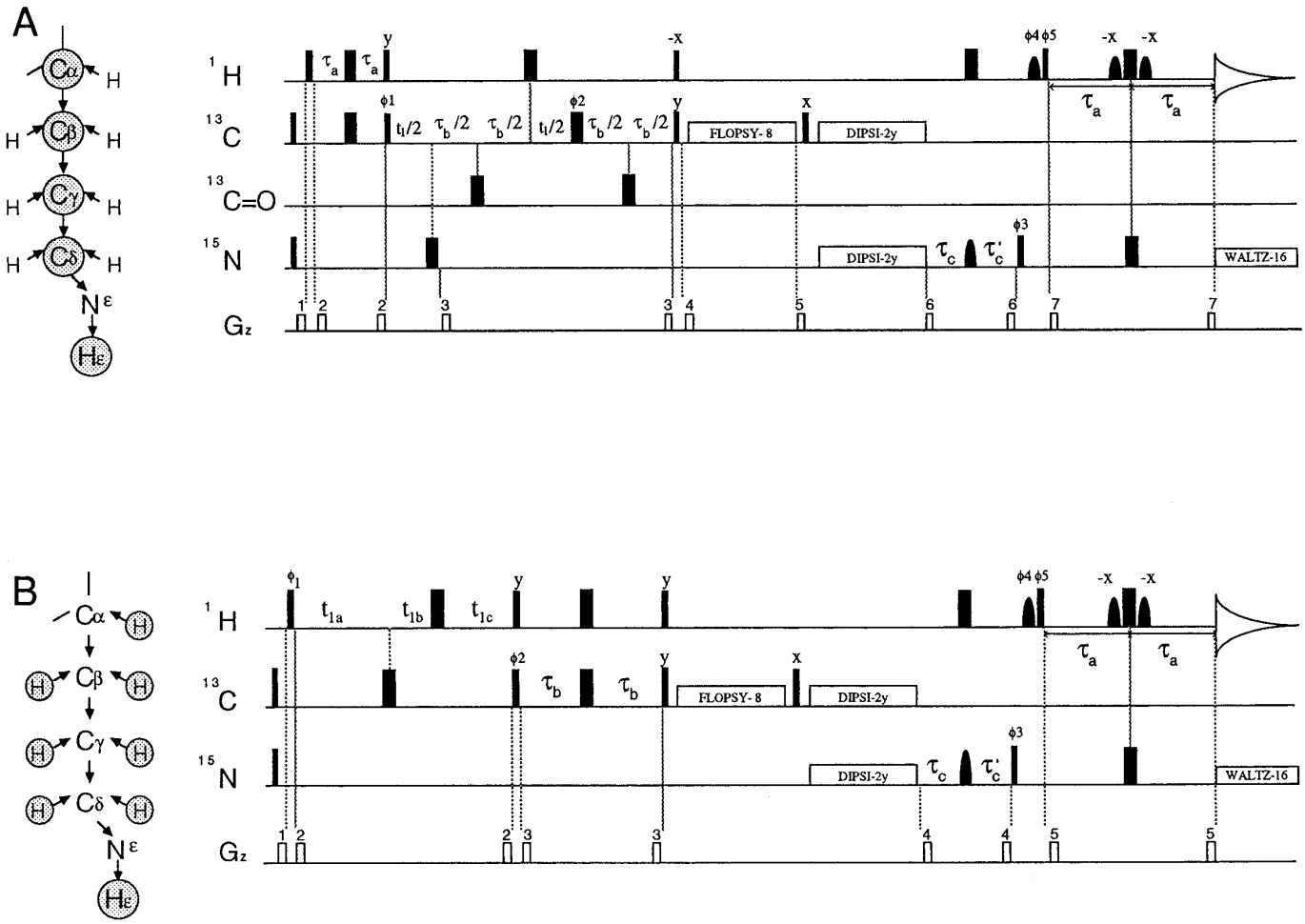

FIG. 2. Pulse sequences for the Arg–(H)C(C)TOCSY–N$^{\epsilon}$H$^{\epsilon}$ (A) and Arg–H(CC)TOCSY–N$^{\epsilon}$H$^{\epsilon}$ (B) experiments. The schematic to the left of each sequence indicates the transfer pathway involved in each experiment. All narrow pulses have a flip angle of 90° and wide pulses a flip angle of 180°. Proton pulses are centered on the water resonance and applied with a field of 28 kHz with the exception of the 2 ms (90°) rectangular ''water-selective'' shaped pulses. The carbon carrier is centered at 43 ppm, and all ^{13}C pulses (i.e., non carbonyl) are applied with a 21 kHz field. The FLOPSY-8 mixing scheme (*17*) employs an 8 kHz field, while a 0.8 kHz field (for both ^{13}C and ^{15}N) is used for hetero-TOCSY transfer (*22, 23*). A DIPSY-2 mixing sequence (*18*) with pulses applied along the $\pm y$ axes is used for the $C^{\delta} \rightarrow N^{\epsilon}$ transfer, with a mixing time of 75 ms. Typically, mixing times of 10–25 ms are employed for the FLOPSY transfer. All ^{15}N pulses prior to the DIPSI mixing are centered at 104 ppm and applied with a 5.5 kHz field. The ^{15}N carrier is switched to 85 ppm immediately after the FLOPSY transfer. Note that the magnetization of interest is along the z axis at this point. The selective refocusing ^{15}N pulse (shaped pulse in the center of the first $2\tau_c$ period) is applied as a 1.4 ms re-SNOB pulse (*24*) with a field strength at maximum amplitude of 1.67 kHz. ^{15}N decoupling during acquisition is achieved with a 1 kHz WALTZ-16 field (*25*). The delays used in the sequence are $\tau_a = 1.7$ ms, $\tau_b = 1.1$ ms, $\tau_c = 2.4$ ms, and $\tau_c' = \tau_c - (2/\pi) \times \mathrm{pw}_n$, where pw_n is the ^{15}N 90° pulse width. (A) The carbonyl pulses are applied as 132 ppm phase-modulated pulses having the SEDUCE-1 profile (*26*) and a length of 250 μs. Quadrature in F_1 is achieved via States–TPPI of $\phi 1$ (*27*). The phase cycle employed is $\phi 1 = x$; $\phi 2 = 2(x), 2(y), 2(-x), 2(-y)$; $\phi 3 = 8(y), 8(-y)$; $\phi 4 = \phi 5 = x, -x$; Rec $= 2(x, -x, -x, -x), 2(-x, x, x, -x)$. The delays and strengths of the gradients are g1 = (1 ms, 5G/cm), g2 = (0.2 ms, 2G/cm), g3 = (0.2 ms, 15 G/cm), g4 = (0.5 ms, 4 G/cm), g5 = (0.3 ms, 6 G/cm), g6 = (0.2 ms, 2.5 G/cm), g7 = (0.1 ms, 10 G/cm). (B) Quadrature in F_1 is achieved via States–TPPI of $\phi 1$ (*27*). The delays t_{1a}, t_{1b}, and t_{1c} are set according to $t_{1a} = t_1/2 + \tau_a$, $t_{1b} = t_1/2 - n\zeta$, and $t_{1c} = \tau_a - n\zeta + 2 \times \mathrm{pw}_c$, where $\zeta = (\tau_a + 2 \times \mathrm{pw}_c - \mathrm{g2})/(N - 1)$ and $n = 0, 1, 2, \cdots N - 1$ (*14, 15*). N is the number of complex acquisition points in t_1 and pw_c is the carbon 90° pulse width. The phase cycle employed is $\phi 1 = 2(x), 2(-x)$; $\phi 2 = 4(x), 4(-x)$; $\phi 3 = 8(y), 8(-y)$; $\phi 4 = \phi 5 = x, -x$; Rec $= x, 2(-x), x, -x, 2(x), -x$. The receiver is inverted every eight scans. The delays and strengths of the gradients are g1 = (1 ms, 5 G/cm), g2 = (0.5 ms, 15 G/cm), g3 = (0.2 ms, 2 G/cm), g4 = (0.4 ms, 12 G/cm), g5 = (0.1 ms, 10 G/cm).

phatic chemical shifts per side chain facilitates the sequential assignment of H$^{\epsilon}$ protons by comparison of these spectra with the H(CCO)NH–TOCSY and (H)C(CO)NH–TOCSY experiments (*14–16*) which correlate side-chain shifts with backbone (^{15}N, NH) spin pairs. Of course, once the H$^{\epsilon}$ shifts are assigned, it is straightforward to link the

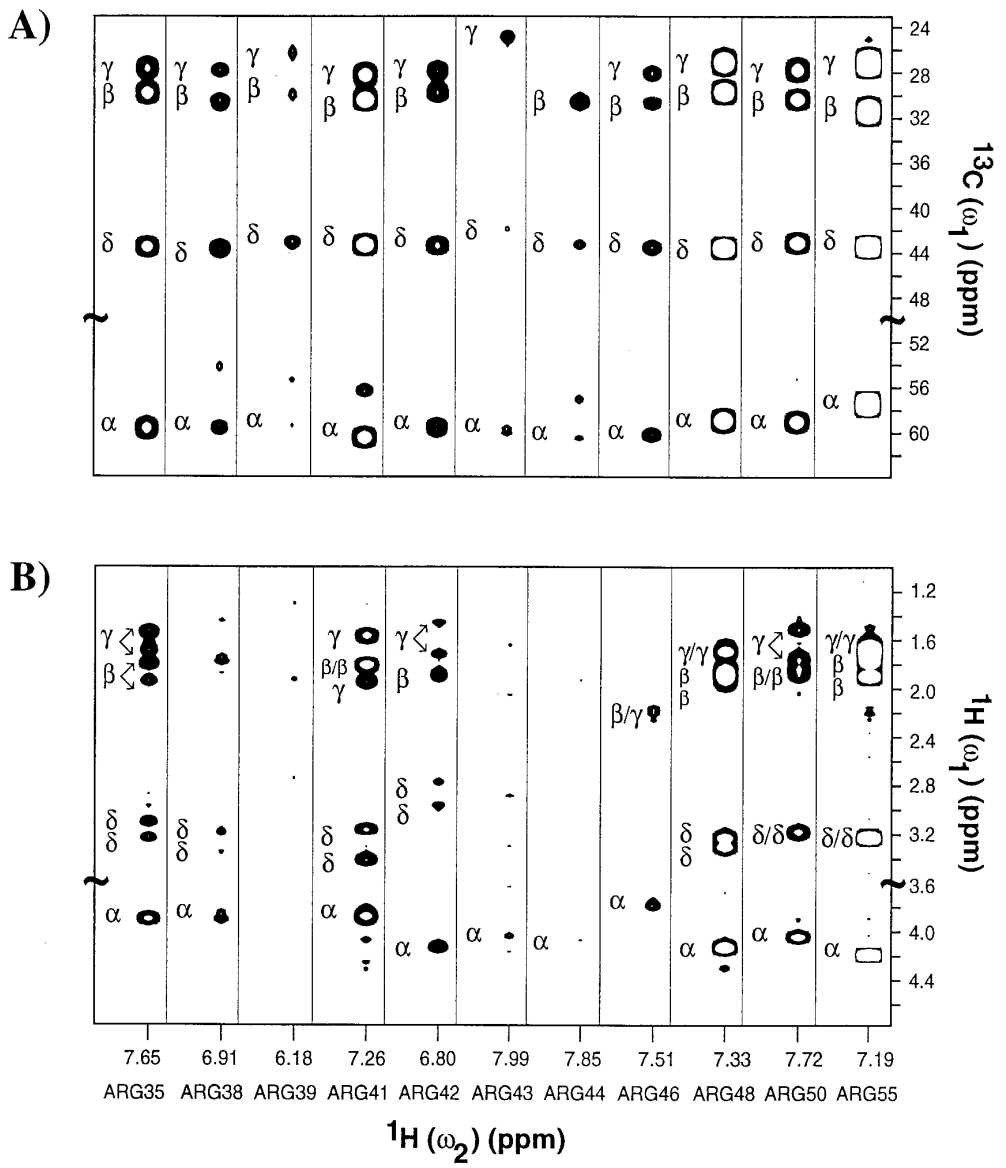

FIG. 3. Strip plots of Arg–(H)C(C)TOCSY–N$^{\epsilon}$H$^{\epsilon}$ (A) and Arg–H(CC)TOCSY–N$^{\epsilon}$H$^{\epsilon}$ (B) spectra showing correlations between side-chain carbon (A) or proton (B) and H$^{\epsilon}$ chemical shifts of arginine residues in a 1:1 complex of a 1.5 m*M* sample of ^{15}N, ^{13}C-labeled HIV-1 Rev peptide–RRE RNA. Note that the peptide is numbered sequentially from 33. Sample conditions were 25°C, 10 m*M* sodium phosphate, 50 m*M* NaCl, 0.1 m*M* EDTA, pH 6.5, 90% H_2O, 10% D_2O. Spectra were acquired on a Varian Unity+ 500 MHz spectrometer equipped with a pulsed-field-gradient unit and a triple-resonance probe with an actively shielded *z* gradient. Arg–(H)C(C)TOCSY–N$^{\epsilon}$H$^{\epsilon}$ and Arg–H(CC)TOCSY–N$^{\epsilon}$H$^{\epsilon}$ spectra were recorded with sweep widths (F_1, F_2) of (7280 Hz, 8000 Hz) and (2100 Hz, 8000 Hz), respectively, and F_1 acquisition times of 8.8 ms (^{13}C) and 30.5 ms (^{1}H). Spectra with homonuclear-TOCSY transfer times of 11.9 and 26.7 ms were recorded, while a heteronuclear TOCSY transfer time of 74.6 ms was employed in each case. Data from the 26.7 ms transfer are illustrated for the α region of each spectrum while the remaining regions are from experiments recorded with 11.9 ms homonuclear transfer times. A recycle delay of 1 s was employed in each experiment and acquisition times of approximately 20 h/spectrum were used.

H$^{\epsilon}$ and H$^{\eta}$ shifts via the Arg–H$^{\eta}$(N$^{\eta}$C$^{\zeta}$N$^{\epsilon}$)H$^{\epsilon}$ experiment that we previously described (*13*). In this regard, the assignment is facilitated by the excellent resolution that generally is present for the H$^{\epsilon}$ spins of arginine side chains. This is shown in Fig. 1, where a portion of the ^{15}N–^{1}H HSQC spectrum of a 1:1 complex of ^{15}N, ^{13}C HIV-1 Rev peptide (23 residues) and RRE RNA (34 nucleotides) is plotted.

Figure 2 illustrates the Arg–(H)C(C)TOCSY–N$^{\epsilon}$H$^{\epsilon}$ (2A) and Arg–H(CC)TOCSY–N$^{\epsilon}$H$^{\epsilon}$ (2B) experiments that were developed to correlate arginine side-chain-carbon

(2A) and -proton (2B) chemical shifts with the H^{ϵ} shift. The experiments employ magnetization-transfer schemes similar to those discussed previously by Yamazaki *et al.* (*13*) and are therefore only briefly described in the present report. In the Arg–(H)C(C)TOCSY-$N^{\epsilon}H^{\epsilon}$ experiment, the flow of magnetization can be schematized as

$$\begin{array}{l} {}^{1}H_i \xrightarrow{J_{HC}} {}^{13}C_i\ (t_1) \xrightarrow{J_{CC}} {}^{13}C^{\delta} \xrightarrow{J_{C^{\delta}N^{\epsilon}}} \\ {}^{15}N^{\epsilon} \xrightarrow{J_{HN}} {}^{1}H^{\epsilon}\ (t_2) \end{array} \qquad [1]$$

with the couplings involved in each transfer indicated above the arrows in [1]; t_1 and t_2 are acquisition times. The transfer pathway is identical for the Arg–H(CC)TOCSY–$N^{\epsilon}H^{\epsilon}$ experiment; in this case, however, the ^1H chemical shift (^1H_i) is recorded during t_1. Transfer of magnetization from the site of origination to the C^{δ} carbon is achieved via a FLOPSY mixing scheme (*17*), with magnetization subsequently relayed to the N^{ϵ} spin via a hetero-TOCSY DIPSI-2 mixing scheme (*18*). Because of the relatively large separation between the chemical shifts of C^{δ} (~43 ppm) and C^{γ} (~28 ppm) carbons it is straightforward to ensure that magnetization proceeds from $C^{\delta} \rightarrow N^{\epsilon}$ with essentially no backtransfer to the C^{γ} position during heteronuclear polarization transfer. Finally, it is worth noting that care has been taken to minimize saturation or dephasing of water magnetization and to ensure that the water is placed along the $+z$ axis immediately prior to detection (*19–21*). This is achieved through the use of water-selective pulses. In addition, in scheme (2A) the proton pulse of phase $(-x)$ applied immediately prior to the FLOPSY mixing places the water magnetization along the $+z$ axis at this point. The action of the gradients g4 and g5 which follow in the pulse sequence will therefore not dephase the water signal.

In scheme (2B), the effect of the ^1H 90°_{y} pulse applied before the FLOPSY period is to ensure that for both cosine and sine t_1 modulated components of the magnetization the water is in the same position immediately prior to carbon mixing. Note that water magnetization resides in the transverse plane after this pulse, and the long transfer times that follow (~10–20 ms and ~75 ms for the homo- and hetero-TOCSY mixing schemes, respectively) allow radiation damping to return the magnetization to the $+z$ axis prior to the application of further proton pulses. In this way, the position of the water signal at the start of acquisition is independent of the phase of proton pulses, and water magnetization is preserved with the same intensity for both *x* and *y* components of the signal. This has been discussed in detail previously (*13*).

Figure 3 illustrates the quality of the data obtained from the pulse schemes presented with strip plots from Arg–(H)C(C)TOCSY–$N^{\epsilon}H^{\epsilon}$ and Arg–H(CC)TOCSY–$N^{\epsilon}H^{\epsilon}$ spectra recorded on the Rev–RRE complex. In general, the Arg–(H)C(C)TOCSY–$N^{\epsilon}H^{\epsilon}$ experiment is more sensitive than its counterpart which records ^1H evolution during t_1, since, for nondegenerate methylene groups, the proton signal is split in two. In practical terms, we have found a combination of Arg–(H)C(C)TOCSY–$N^{\epsilon}H^{\epsilon}$ and (H)C(CO)NH–TOCSY experiments (*14–16*) to be extremely useful in establishing the sequential assignments of arginine H^{ϵ} through a comparison of side-chain-carbon chemical shifts provided in both experiments. It is of interest to note that of the three weakest sets of correlations in Fig. 3 (Arg 39, 43, and 44) both Arg 39 and 44 make contacts with bases in the major groove of the RNA, while Arg 43 makes multiple contacts with both sugar and phosphate groups of G71 and U72 on the RNA (*4*). Relaxation studies of Arg–N^{ϵ} nitrogens indicate that these three arginines have significantly larger order parameters than their counterparts.

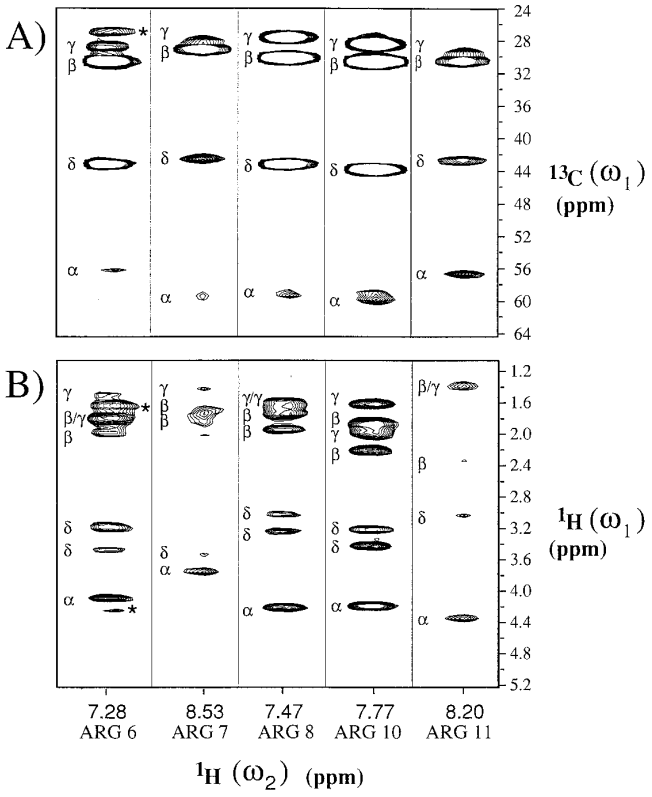

FIG. 4. Strip plots of Arg–(H)C(C)TOCSY–$N^{\epsilon}H^{\epsilon}$ (A) and Arg–H(CC)TOCSY–$N^{\epsilon}H^{\epsilon}$ (B) spectra recorded on a 2.9 m*M* sample of an ^{15}N, ^{13}C peptide (24 amino acids) from the bacteriophage λ N protein in 1:1 complex with boxB RNA (19 nucleotides) (*8*). Sample conditions were 25°C, 25 m*M* d_4-succinate, 100 m*M* NaCl, 0.2 m*M* EDTA, 0.05 m*M* NaN_3, pH 5.5, 90% H_2O, 10% D_2O. Spectra were recorded as described in the legend of Fig. 3. A homonuclear transfer time of 14.8 ms was employed, while the $^{13}C^{\delta} \rightarrow {}^{15}N$ transfer was allowed to proceed for 74.6 ms. Signals from ~1% unbound peptide are indicated with *.

Analogous plots of spectra recorded on a 2.9 m*M* sample of an ^{15}N, ^{13}C peptide (24 amino acids) from the amino terminus of bacteriophage λ N protein in 1:1 complex with boxB RNA (19 nucleotides) (*8*) are shown in Fig. 4. Complete sequential assignments of arginine H^{ϵ}'s have been obtained, and we are now in the process of determining a three-dimensional structure of the complex.

In summary, pulse schemes have been presented for the sequential assignment of arginine H^{ϵ} spins. The experiments have been applied to two RNA–peptide complexes under study in our laboratories. The combination of these experiments and existing sequences for correlating side-chain-carbon and backbone-amide shifts has facilitated assignment of H^{ϵ} spins in molecular complexes containing large numbers of arginines and where assignment of these residues is absolutely crucial for accurate structure determinations.

ACKNOWLEDGMENTS

This research was supported by grants from the Natural Sciences and Engineering Research Council of Canada (L.E.K.), the Medical Research Council of Canada (J.G.), the Searle Scholars Program of the Chicago Community Trust (J.R.W.), and the National Institutes of Health GM-53320 (J.R.W.). P.L. is a Terry Fox Research Fellow of the National Cancer Institute of Canada supported with funds provided by the Terry Fox Run. J.G. is an International Research Scholar of the Howard Hughes Medical Institute.

REFERENCES

1. A. Bax and S. Grzesiek, *Acc. Chem. Res.* **26,** 131 (1992).
2. J. D. Puglisi, L. Chen, S. Blanchard, and A. D. Frankel, *Science* **270,** 1200 (1995).
3. F. H. T. Allain, C. C. Gubser, P. W. A. Howe, K. Nagai, D. Neuhaus, and G. Varani, *Nature* **380,** 646 (1996).
4. J. L. Battiste, H. Mao, N. S. Rao, R. Tan, D. R. Muhandiram, L. E. Kay, A. D. Frankel, and J. R. Williamson, *Science* **273,** 1547 (1996).
5. N. Pavletich and C. O. Pabo, *Science* **252,** 809 (1991).
6. J. Janin, S. Miller, and C. Chothia, *J. Mol. Biol.* **204,** 155 (1988).
7. D. Lazinski, E. Grzadzielska, and A. Das, *Cell* **59,** 207 (1989).
8. R. Tan and A. D. Frankel, *Proc. Natl. Acad. Sci. USA* **92,** 5282 (1995).
9. N. T. Mrabet, A. Van den Broeck, I. Van den brande, P. Stanssens, Y. Laroche, A. M. Lambeir, G. Matthijssens, J. Jenkins, M. Chiadmi, H. van Tilbeurgh, F. Rey, J. Janin, W. J. Quax, I. Lasters, M. De Maeyer, and S. J. Wodak, *Biochemistry* **31,** 2239 (1992).
10. T. Yamazaki, M. Yoshida, and K. Nagayama, *Biochemistry* **32,** 5656 (1993).
11. M. Wittekind, W. J. Metzler, and L. Mueller, *J. Magn. Reson. B* **101,** 214 (1993).
12. H. Vis, R. Boelens, M. Mariani, R. Stroop, C. E. Vorgias, K. S. Wilson, and R. Kaptein, *Biochemistry* **33,** 14,858 (1994).
13. T. Yamazaki, S. M. Pascal, A. U. Singer, J. D. Forman-Kay, and L. E. Kay, *J. Am. Chem. Soc.* **117,** 3556 (1995).
14. S. Grzesiek and A. Bax, *J. Biomol. NMR* **3,** 185 (1993).
15. T. M. Logan, E. T. Olejniczak, R. X. Xu, and S. W. Fesik, *J. Biomol. NMR* **3,** 225 (1993).
16. G. T. Montelione, B. A. Lyons, S. D. Emerson, and M. Tashiro, *J. Am. Chem. Soc.* **114,** 10,974 (1992).
17. M. Kadkhodaie, O. Rivas, M. Tan, A. Mohebbi, and A. J. Shaka, *J. Magn. Reson.* **91,** 437 (1991).
18. A. J. Shaka, C. J. Lee, and A. Pines, *J. Magn. Reson.* **77,** 274 (1988).
19. S. Grzesiek and A. Bax, *J. Am. Chem. Soc.* **115,** 12,593 (1993).
20. J. Stonehouse, G. L. Shaw, J. Keeler, and E. Laue, *J. Magn. Reson. A* **107,** 178 (1994).
21. L. E. Kay, G. Y. Xu, and T. Yamazaki, *J. Magn. Reson. A* **109,** 129 (1994).
22. D. W. Bearden and L. R. Bron, *Chem. Phys. Lett.* **163,** 432 (1989).
23. E. R. P. Zuiderweg, *J. Magn. Reson.* **89,** 533 (1990).
24. E. Kupce, J. Boyd, and I. D. Campbell, *J. Magn. Reson. B* **106,** 300 (1995).
25. A. J. Shaka, J. Keeler, T. Frenkiel, and R. Freeman, *J. Magn. Reson.* **52,** 335 (1983).
26. M. McCoy and L. Mueller, *J. Am. Chem. Soc.* **114,** 2108 (1992).
27. D. Marion, M. Ikura, R. Tschudin, and A. Bax, *J. Magn. Reson.* **85,** 393 (1989).